Available online at www.sciencedirect.com

ScienceDirect

Polymer 47 (2006) 6874–6879

polymer

www.elsevier.com/locate/polymer

Flame retardant nanocomposites of polyamide 6/clay/silicone rubber with high toughness and good flowability

Weifu Dong [a,b], Xiaohong Zhang [b], Yiqun Liu [b], Qingguo Wang [a,b], Hua Gui [a,b], Jianming Gao [b], Zhihai Song [b], Jinmei Lai [b], Fan Huang [b], Jinliang Qiao [b,*]

[a] *College of Materials Science and Engineering, Beijing University of Chemical Technology, Beijing 100029, People's Republic of China*
[b] *SINOPEC Beijing Research Institute of Chemical Industry, No. 14, Beisanhuan Donglu, Chao Yang, Beijing 100013, People's Republic of China*

Received 22 March 2006; received in revised form 3 July 2006; accepted 5 July 2006
Available online 8 August 2006

Abstract

A novel flame retardant, silicone elastomeric nanoparticle (S-ENP) with T_g of -120 °C and particle size of ~ 100 nm has been developed and used as a modifier for polyamide 6 (nylon-6). It has been found that S-ENP can not only increase the toughness and improve the flame retardancy of nylon-6 but also helps unmodified clay exfoliate in nylon-6 matrix. It has been also found that the S-ENP and exfoliated clay platelet in nylon-6 have a synergistic flame retardant effect on nylon-6. A novel flame retardant nanocomposite of nylon-6/unmodified clay/S-ENP with high toughness, high heat resistance, high stiffness and good flowability has been prepared and a mechanism of synergistic flame retardancy has also been proposed.

Keywords: Clay; Flame retardancy; Silicone

1. Introduction

In recent years, more and more environmental legislations have limited or prohibited the application of halogen-containing flame retardants in polymer materials. Considerable research has been focused on inorganic fillers and organosilicones as halogen-free flame retardants [1–5]. However, inorganic flame retardants are usually less effective and the addition level of up to 60 wt% is normally required in order to achieve acceptable resistance to combustion [3]. Such high level addition will in turn lead to deteriorated toughness and processability [3,6]. Some elastomers could be used to improve the toughness of flame retardant plastics [6,7], but makes the processability even worse. Recently, a new flame retardant approach via polymer/clay nanocomposites has attracted a great deal of interest, because the addition of small amount clay brings out a large reduction in the peak heat release rate (PHRR) using a cone calorimeter [8–15]. The PHRR is vital to the evaluation of the fire safety of material [16], because this give a measure of the size of fire. However, the polymer/clay nanocomposites are usually more brittle than pure polymer and organic modification of clay makes the manufacturing process of polymer/clay nanocomposites costly [17–26]. The organosilicone can only be used in aromatic thermoplastics, such as polycarbonate, polystyrene and acrylonitrile–butadiene–styrene copolymer (ABS), and also decreases the toughness and stiffness of thermoplastics [4,5]. Needless to say that a composite with good flame retardancy, balanced mechanical properties and good processability is much desired, but extremely hard to achieve.

In this study, based on a novel elastomeric flame retardant, the silicone elastomeric nanoparticle (S-ENP) with T_g of -120 °C [27,28], a flame retardant polyamide 6 (nylon-6) nanocomposite with high toughness, high heat resistant, high stiffness and good flowability has been prepared. It was found that the S-ENP with average particle size of 100 nm was

---

* Corresponding author. Tel.: +86 10 59202375; fax: +86 10 64228661.
E-mail address: jqiao@brici.ac.cn (J. Qiao).

0032-3861/$ - see front matter © 2006 Elsevier Ltd. All rights reserved.
doi:10.1016/j.polymer.2006.07.038

effective in improving flame retardancy and toughness of nylon-6 and can also help unmodified clay to be exfoliated in nylon-6 matrix. On the basis of clay slurry and S-ENP latex, another novel elastomeric flame retardant of S-ENP/clay (S-ENPC) was produced. It was found that the S-ENP and clay platelets in S-ENPC had a synergistic flame retardant effect on nylon-6, which resulted in the further enhancement of flame retardancy of the nylon-6. Furthermore, nylon-6/S-ENPC nanocomposites exhibited not only high toughness, stiffness and heat distortion temperature but also low melt viscosity.

2. Experimental section

2.1. Materials and sample preparation

The nylon-6 used in this study is commercially available from BASF (Ultramid B4) with $\overline{M_n} = 33{,}000$. Silicone latex (KH-L10, solid content: 30 wt%; average single latex particle size, ca 100 nm) was produced by Beijing Kehua Inc. S-ENP was prepared by spray drying the irradiated silicone latex according to patent technology [27,28]. POE-*g*-MAH (493D) was purchased from Dupont Corporation. Sodium montmorillonite (Na-MMT), with cation exchange capacity (CEC) of 90 meq/100 g was purchased from Zhangjiakou Qinghe Chemical Plant, China.

S-ENP and S-ENPC were prepared by the method schematically shown in Fig. 1. The raw material for producing S-ENP was common silicone latex. After premixed with cross-linking agent, the silicone latex was irradiated with γ ray and changed into highly cross-linked rubber particle with much higher cross-linking degree on the particle surface [29,30]. S-ENP was finally produced by spray drying the highly cross-linked rubber latex. The preparation of S-ENPC is similar to that of S-ENP. Firstly, clay powder was dispersed into water by using an emulsifier for 30 min to form a clay slurry containing 2 wt% of clay. The highly cross-linked silicone rubber latex was added into the clay slurry at a dry weight ratio of 4/1 and stirred for 60 min to form a uniform mixture, in which the clay platelets and the cross-linked silicone rubber particles were interpenetrated. S-ENPC can be obtained after spray drying the mixture. After spray drying, the special microstructure that S-ENP particles and exfoliated clay platelets partitioned each other was retained in S-ENPC. The nylon-6/S-ENPC nanocomposites were prepared by using a conventional co-rotating twin-screw extruder. During melt blending, the exfoliated clay platelets are hardly aggregated due to the partitioning effect of S-ENP. Two nylon-6 nanocomposites with S-ENP and S-ENPC were prepared (see Table 1 for their specific compositions).

Table 1
The composition of nylon-6 composites

Sample code	Composition (wt)			
	Nylon-6	S-ENP	S-ENPC (S-ENP/clay = 4/1, wt/wt)	POE-*g*-MAH
PA-1	100	10	–	–
PA-2	100	–	10	–
PA-3	100	–	–	10

Nylon-6 nanocomposites were compounded according to the following process: nylon-6, S-ENPC (S-ENP or POE-*g*-MAH) and Irganox 1010 (0.3 wt%, as stabilizer) were mixed in a high-speed mixer at a certain weight ratio. The mixture was then fed into a co-rotating twin-screw extruder (ZSK-25, Werner and Pleiderer, $L/D = 30$) at a barrel temperature of 250 °C, a screw speed of 300 rpm, and a feed rate of 10 kg/h. In addition, prior to mixing, PA6 and S-ENPC (or S-ENP) were dried at 100 °C and 80 °C, respectively for 6 h in an air oven.

The extruded composite pellets were injection molded to obtain specimens for various mechanical tests with the following specifications: tensile strength test (ASTMD-638, Type I), impact strength test (ASTMD-256, $127 \times 12.7 \times 6.4\ \text{mm}^3$), flexural strength test (ASTMD-790, $127 \times 12.7 \times 3.2\ \text{mm}^3$), and heat distortion temperature (HDT) test (ASTMD-648, $127 \times 12.7 \times 6.4\ \text{mm}^3$). Test specimens were prepared by injection molding with a barrel temperature of 250 °C, molding temperature of 80 °C, injection pressure of 4.5 MPa, and a holding pressure of 4.0 MPa.

2.2. Measurements and characterization

Mechanical properties. Tensile and flexural tests were conducted by using an Instron model 4466 testing machine according to ASTMD-638 and ASTMD-790, respectively. Notched Izod impact test was performed by using a CEAST impact machine according to ASTMD-256. HDT was tested

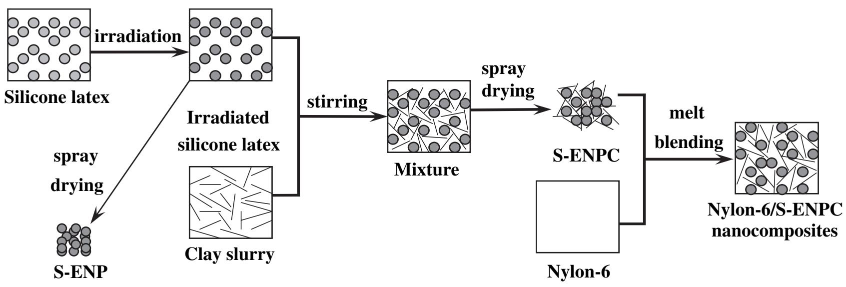

Fig. 1. Schematic diagram of the preparation of S-ENP and nylon-6/S-ENPC nanocomposites. The solid gray and black circles represent the silicone latex particle and S-ENP. The black lines correspond to exfoliated clay platelets.

with an HD-PC Heat Distortion Tester according to ASTMD-648.

Morphology observation. The morphology of silicate layers in nylon-6 composites was observed by using transmission electron microscopy (TEM) (Philips TECNAI 20). The ultra-thin sections, 50–100 nm in thickness, were cryotomed from injection molded specimens at −80 °C.

X-ray diffraction (*XRD*). XRD was conducted by using a SHIMADZU D/Max 2500VB2+/PC diffractometer. XRD scans were obtained in reflection mode by using an incident X-ray wavelength of 0.1542 nm at a scan rate of 1.0 deg/min.

Thermogravimetric analysis (*TGA*). TGA was carried out at a heating rate of 10 °C/min under nitrogen flow of 50 ml/min by a thermogravimetric analyzer TGA 7 (Perkin Elmer, US).

Cone calorimeter testing. The samples were exposed to a Fire Test Technology Cone Calorimeter according to ISO5660 at an external heat flux of 35 kW/m^2. The specimens prepared by compression molding were plates of $100 \times 100 \times 4$ mm^3. Heat release rate (HRR), peak heat release rate (PHRR), effective heat combustion (EHC), and other quantifiable parameters including carbon dioxide, carbon monoxide and specific extinction area (SEA) were recorded.

Energy-dispersive spectrometer (*EDS*). Si, O, Al, C, and other element content in the collected sample residues were measured by EDS instrument (Thermo NORAN, US).

Rheology measurements. Shear viscosities were measured at 250 °C by using a Rheograph 2001 Capillary Rheometer (GOETTFERT) equipped with a capillary die having a diameter of 1 mm and a length of 10 mm. Capillary data were corrected by using the Rabinowitsch–Mooney relationship in order to obtain true shear viscosities.

Glass transition temperature (T_g). The glass transition temperature (T_g) was measured by means of differential scanning calorimetry (DSC) (TA Q100) at a heating rate of 10 °C/min.

3. Results and discussion

The flammability properties of nylon-6 composites were characterized by means of cone calorimetry. The heat release rate (HRR) plots for pure nylon-6, PA-1 and PA-2 at 35 kW/m^2 heat flux are shown in Fig. 2 and some cone calorimetry data are listed in Table 2. It can be seen that the PA-1 shows a 60% lower peak heat release rate (PHRR) compared to pure nylon-6, which indicates that the addition of S-ENP can significantly decrease the flammability of nylon-6. Furthermore, the PHRR of PA-2 is 68% lower than that of nylon-6, even lower than that of PA-1. The similar trends are seen for mean HRR. It is obvious that S-ENPs and exfoliated clay platelets in S-ENPC exhibit a synergistic flame retardant effect on nylon-6. Moreover, the shift of peak HRR from 375 s for nylon-6 to 685 s PA-1 suggests the time to reach the peak HRR is largely improved for PA-1. As for PA-2, the time to peak HRR (380 s) is similar to that of nylon-6. This behavior may be explained by TGA analysis.

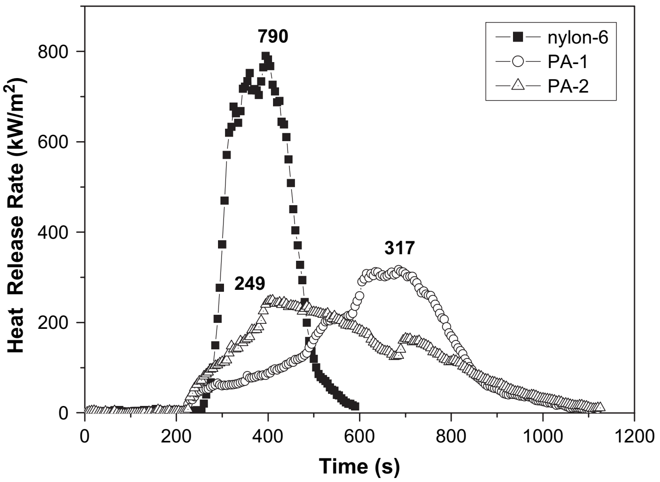

Fig. 2. Heat release rate (HRR) plots for pure nylon-6, PA-1 and PA-2 at a heat flux of 35 kW/m^2.

The TGA curves of nylon-6, PA-1 and PA-2 in nitrogen are shown in Fig. 3. We found that the decomposition temperature of the nylon-6 composites does not vary significantly from that of pure nylon-6, a small increase for PA-1 (425 °C) and decrease for PA-2 (420 °C) compared to pure nylon-6 (424 °C). However, the TGA curve of PA-1 shifts to high

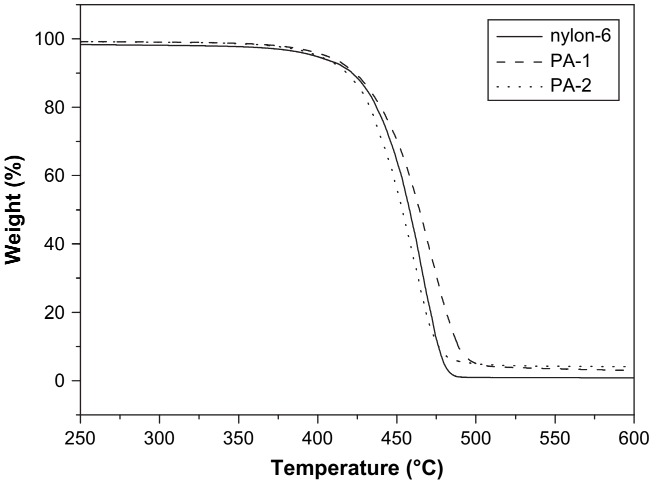

Fig. 3. TGA curves of nylon-6, PA-1 and PA-2 in N$_2$ at 10 °C/min.

Table 2
Cone calorimeter data at a heat flux of 35 kW/m^2

Samples	Peak HRR (kW/m^2) (Δ%)	Mean HRR (kW/m^2) (Δ%)	Time to peak HRR (s)	Mean EHC (MJ/kg)	Mean SEA (m^2/kg)	Mean CO yield (kg/kg)	Mean CO$_2$ yield (kg/kg)
Nylon-6	790	370	375	26	179	0.02	2
PA-1	317 (60)	129 (65)	685	25	275	0.02	2
PA-2	249 (68)	110 (70)	380	24	262	0.03	3

Table 3
Mechanical properties of pure nylon-6 and nylon-6 composites

Sample code	Elongation at break (%)	Notched Izod impact strength (J/m) 23 °C	Notched Izod impact strength (J/m) −20 °C	Flexural modulus (GPa)	Heat distortion temperature (°C)
Nylon-6	51	41.2	34.9	2.44	54.0
PA-1	55	71.9	54.4	2.27	54.1
PA-2	72	74.7	61.6	2.71	61.8

temperature evidently compared to that of nylon-6 after the beginning of decomposition, which is correlated to an improvement of the time to peak HRR of PA-1. And the close TGA curves of PA-2 and nylon-6 relate their similar time to peak HRR.

The mechanical properties of nylon-6 composites are shown in Table 3. It can be seen that PA-2, a nylon-6/S-ENPC nanocomposite, exhibits not only higher flexural modulus and heat distortion temperature but also higher impact strength and elongation compared with pure nylon-6 and PA-1.

PA-2 also has excellent flowability, as can be seen in Fig. 4. It can be seen that the PA-2 shows a viscosity almost as same as that of PA-1 and much lower than PA-3, nylon-6/POE-*g*-MAH blends as control sample. Furthermore, PA-2 exhibits a lower melt viscosity than pure nylon-6 at most shear rate region. The results suggest that PA-2, a nylon-6/S-ENPC nanocomposite, has better processability than pure nylon-6 in most of the applications.

It is obvious that the new nylon-6/S-ENPC nanocomposite has good flame retardant property, high toughness and excellent processability. It is interesting to know how the material can achieve such comprehensive property.

Fig. 5 (a and b) shows X-ray diffraction (XRD) patterns of clay and S-ENPC. The clay exhibits an apparent peak at $2\theta = 7.1°$ corresponding to 001 diffraction peak. The interlayer spacing of clay is 1.25 nm. On the other hand, there is no peak in XRD pattern of the S-ENPC, which indicates that the silicate layers of clay in S-ENPC are stacked irregularly. That is to say that the S-ENPs and exfoliated clay platelets partition each other in S-ENPC. The silicate layers are also exfoliated in nylon-6 matrix since no peak can be seen in the XRD pattern of nylon-6/S-ENPC nanocomposites. TEM micrographs conformed XRD result as shown in Fig. 6.

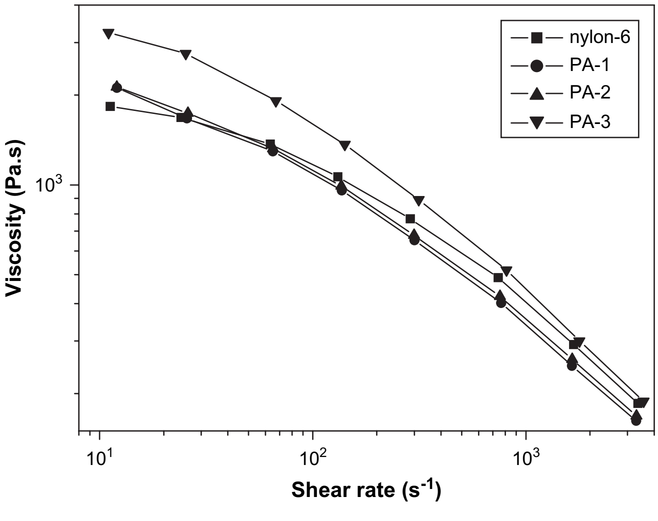

Fig. 4. Shear viscosity versus shear rate from a capillary rheometer at 250 °C for pure nylon-6, PA-1, PA-2 and PA-3.

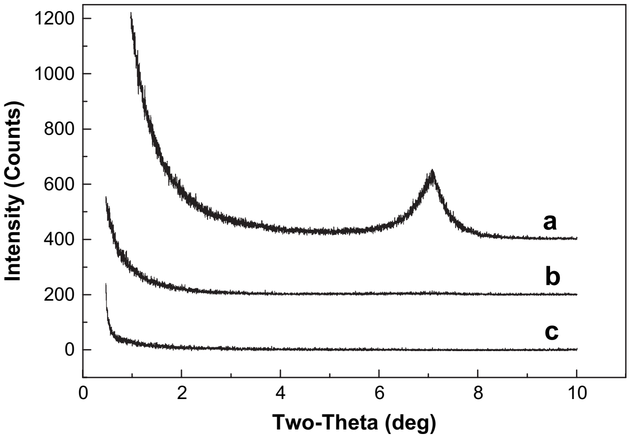

Fig. 5. X-ray diffraction patterns of (a) clay, (b) S-ENPC and (c) PA-2.

It is well known that exfoliated clay can increase the polymer's stiffness and heat resistance, and rubbers can raise plastics' toughness. Furthermore, the silicone rubber can also be a flowability modifier for plastics since it contains —Si—O—R— group.

As for the mechanism of flame retardancy, it has been found that the source of the improved flammability is due to the differences in condensed-phase decomposition process rather than a gas-phase [8]. We found that, the same as shown in Table 2, the mean effective heat combustion (EHC), mean carbon dioxide yield, mean carbon monoxide yield of composites are similar to pure nylon-6.

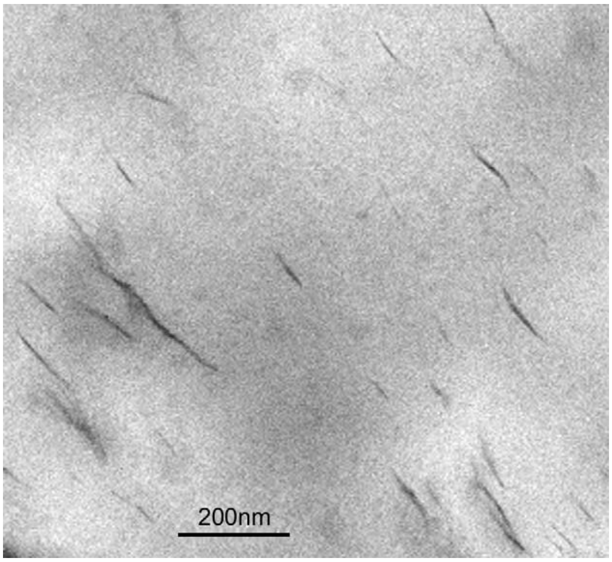

Fig. 6. TEM image of PA-2 (nylon-6/S-ENPC).

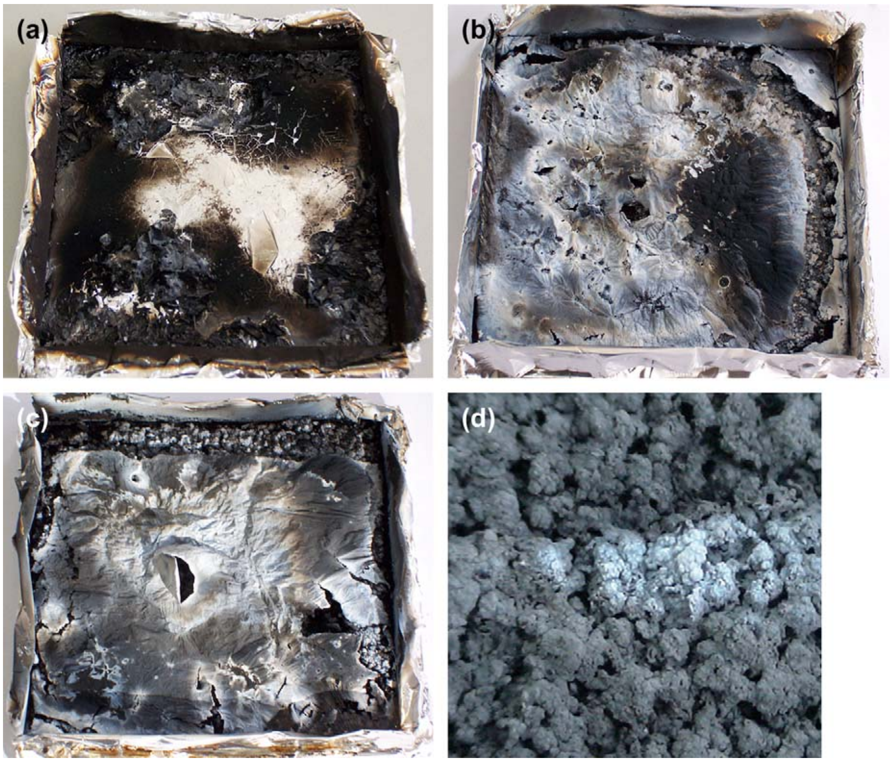

Fig. 7. Digital pictures of residue surface of pure nylon-6 (a), PA-1 (b), PA-2 (c) and island-like floccules of the PA-2 residues (d) at the end of the combustion.

The only difference was found in the process of cone calorimetric measurement. While pure nylon-6 had a boiling surface, a coat-like layer was formed on the surface of the PA-1 and PA-2 before ignition. Whereas pure nylon-6 left almost no residue at the end of combustion (Fig. 7a), PA-1 retained a white coat-layer (Fig. 7b) on the surface of the residue and some white powder underneath. Besides a white coat-layer, PA-2 (Fig. 7c) left some island-like floccules underneath (Fig. 7d), which are similar to the floccules reported by Kashiwagi et al. on nylon-6/clay nanocomposites [15]. Covering most sample surface, the coat-like layer composed of silica as shown in Table 4 can insulate the underlying material and delay the mass loss of decomposition; therefore, the formation of coat-like layer leads to a significant reduction in flammability, which is similar to the results from the polycarbonate/silicone derivative blends [4]. The island-like floccules in PA-2 composed of silica and clay as shown in Table 4 also play a role of insulation layer as existed in nylon-6/clay nanocomposites [15]. It is obvious that the two barrier layers result in a synergistic flame retardant effect on nylon-6; therefore, PA-2 has an even better flame retardancy than PA-1.

Table 4
Element contents in the portion of residues collected at the end of the cone calorimeter test

Portions of the residue	Si (atom%)	O (atom%)	Al (atom%)	C (atom%)	Na, Mg, Fe (atom%)
Surface of coat-like layer (PA-1)	37.27	62.73	–	–	–
Surface of coat-like layer (PA-2)	36.93	63.07	–	–	–
Surface of island-like floccules (PA-2)	40.67	59.16	0.17	–	–
Bottom of island-like floccules (PA-2)	26.74	56.07	1.97	13.89	1.33

4. Conclusion

In conclusion, two novel halogen-free, elastomeric flame retardants for polymer, S-ENP and S-ENPC, have been developed and used for nylon-6 modification. Besides good flame retardancy, the nylon-6/S-ENPC nanocomposites exhibit high toughness, stiffness and heat distortion temperature, as well as low melt viscosity. It is found that the S-ENP and clay in S-ENPC have a synergistic flame retardant effect on nylon-6 resulting from the formation of two barriers, coat-like layer and island-like floccules, on the nanocomposite residue surface at the end of combustion.

Acknowledgements

This research was subsidized by the Special State Funds for Major Basic Research Projects 2005CB623805.

References

[1] Hornsby PR. Inter Mater Rev 2001;46:199–210.
[2] Miyata S, Imahshi T, Anabuki H. J Appl Polym Sci 1980;25:415.
[3] Hornsby PR, Watson CL. Plast Rubber Process Appl 1989;11:45–51.
[4] Iji Masatoshi, Serizawa Shin. Polym Adv Technol 1998;9:593–600.

[5] Ebdon JR, Hunt BJ, Jones MS, Thorpe FG. Polym Degrad Stab 1996;54:395–400.

[6] Wang J, Tung JF, Ahmed Fuad MY, Hornsby PR. J Appl Polym Sci 1996;60:1425–37.

[7] Wang Z, Shen X, Fan W, Hu Y, Qu B, Gui Z. Polym Int 2002;51:653–7.

[8] Gilma JW, Jackson CL, Morgan AB, Harris Jr R, Manias E, Giannelis EP, et al. Chem Mater 2000;12:1866–73.

[9] Beyer G. Fire Mater 2001;25:193–7.

[10] Zanetti M, Camino G, Mülhaupt R. Polym Degrad Stab 2001;74:413–7.

[11] Zhu J, Uhl FM, Morgan AB, Wilkie CA. Chem Mater 2001;13:4649–54.

[12] Jang BN, Wilkie CA. Polymer 2005;46:3264–74.

[13] Zhu J, Start P, Mauritz A, Wilkie CA. Polym Degrad Stab 2002;77:253–8.

[14] Dabrowski F, Bourbigot S, Delobel R, Le Bras M. Eur Polym J 2000;36:273–84.

[15] Kashiwagi Takashi, Harris Jr Richard H, Zhang Xin, Briber RM, Cipriano Bani H, Raghavan Srinivasa R, et al. Polymer 2004;45:881–91.

[16] Babrauskas V, Peacock RD. Fire Saf J 1992;18(3):255–72.

[17] Vaia RA, Vasudevan S, Kraviec W, Scanlon LG, Giannelis EP. Adv Mater 1995;7:154–6.

[18] (a) Usuki A, Kawasumi M, Kojima Y, Fukushima Y, Okada A, Kurauchi T, et al. J Mater Res 1993;8:1179–84;
(b) Kojima Y, Usuki A, Kawasumi M, Fukushima Y, Okada A, Kurauchi T, et al. J Mater Res 1993;8:1185–9.

[19] (a) Liu L, Qi Z, Zhu X. J Appl Polym Sci 1999;71:1133–8;
(b) Cho JW, Paul DR. Polymer 2001;42:1083–94.

[20] Hasegawa N, Okamoto H, Kato M, Usuki A, Sato N. Polymer 2003;44:2933–7.

[21] Vaia RA, Isii H, Giannelis EP. Chem Mater 1993;5:1694–6.

[22] Wang MS, Pinnavaia TJ. Chem Mater 1994;6:468–74.

[23] Pattanayak Asim, Jana Sadhan C. Polymer 2005;46(10):3275–88.

[24] Cao Xia, James Lee L, Widya Tomy, Macosko Christopher. Polymer 2005;46(3):775–83.

[25] Choi Woo Jin, Kim Se Hoon, Kim Young Jin, Kim Sung Chul. Polymer 2004;45(17):6045–57.

[26] Sheng N, Boyce MC, Parks DM, Rutledge GC, Abes JI, Cohen RE. Polymer 2004;45(2):487–506.

[27] Qiao J, Wei G, Zhang X, Zhang S, Gao J, Zhang W, et al. US Patent 6423760; 2002.

[28] Zhang X, Qiao J, Wei G, Gao J, Liu Y, Zhang S, et al. US Patent 6838490; 2005.

[29] Liu Y, Zhang X, Wei G, Gao J, Huang F, Zhang M, et al. Chin J Polym Sci 2002;20:93–8.

[30] Huang F, Liu Y, Zhang X, Gao J, Song Z, Tan B, et al. Sci China Ser B (Chem) 2004;34:432–40.